



This is a repository copy of *Forecasting the severity of the Newfoundland iceberg season using a control systems model*.

White Rose Research Online URL for this paper:
<https://eprints.whiterose.ac.uk/148565/>

Version: Accepted Version

Article:

Bigg, G.R. orcid.org/0000-0002-1910-0349, Zhao, Y. and Hanna, E. orcid.org/0000-0002-8683-182X (2019) Forecasting the severity of the Newfoundland iceberg season using a control systems model. *Journal of Operational Oceanography*, 14 (1). pp. 24-36. ISSN 1755-876X

<https://doi.org/10.1080/1755876x.2019.1632128>

This is an Accepted Manuscript of an article published by Taylor & Francis in *Journal of Operational Oceanography* on 20th June 2019, available online:
<http://www.tandfonline.com/10.1080/1755876X.2019.1632128>.

Reuse

Items deposited in White Rose Research Online are protected by copyright, with all rights reserved unless indicated otherwise. They may be downloaded and/or printed for private study, or other acts as permitted by national copyright laws. The publisher or other rights holders may allow further reproduction and re-use of the full text version. This is indicated by the licence information on the White Rose Research Online record for the item.

Takedown

If you consider content in White Rose Research Online to be in breach of UK law, please notify us by emailing eprints@whiterose.ac.uk including the URL of the record and the reason for the withdrawal request.



eprints@whiterose.ac.uk
<https://eprints.whiterose.ac.uk/>

Forecasting the severity of the Newfoundland iceberg season using a control systems model

Grant R. Bigg^a, Yifan Zhao^b, Edward Hanna^c

^aDepartment of Geography, University of Sheffield, Sheffield, UK; ^bSchool of Aerospace, Transport and Manufacturing, Cranfield University, Cranfield, UK; ^cSchool of Geography and Lincoln Centre for Water & Planetary Health, University of Lincoln, Lincoln, UK

Grant R. Bigg, grant.bigg@sheffield.ac.uk; Department of Geography, University of Sheffield, Sheffield S10 2TN, UK

Forecasting the severity of the Newfoundland iceberg season using a control systems model

The iceberg hazard for the Grand Banks area to the east of Newfoundland varies dramatically from one year to the next. In some years no icebergs penetrate south of 48°N, while in others well over 1000 icebergs enter the main shipping lanes between Europe and NE North America. Advance knowledge of this seasonal hazard would have major implications for ship routing, as well as the resources required for maintaining an effective ice hazard service. Here, a Windowed Error Reduction Ratio control system identification approach is used to forecast the severity of the 2018 iceberg season off Newfoundland, in terms of the predicted number of icebergs crossing 48°N, as well as to hindcast iceberg numbers for 2017. The best estimates are for 766 ± 297 icebergs crossing 48°N before the end of September 2017 and 685 ± 207 for 2018. These are both above the recent observed average of 592 icebergs for that date, and substantially so for 2017. Given the bimodal nature of the annual iceberg number, this means that our predictions for both 2017 and 2018 are for a high iceberg season, with a 71% level of confidence. However, it is most likely that the 2018 iceberg numbers will be somewhat less than 1000, while our higher hindcast for 2017 is consistent with the observed level of 1008. Our verification analysis, covering the 20-year period up to 2016, shows our model's correspondence to the high or low nature of the 48°N iceberg numbers is statistically robust to the 0.05 % level, with a skill level of 80%.

Keywords: iceberg hazard; Newfoundland; control systems model; prediction; Labrador Current; windowed error reduction ratio

1. Introduction

Ever since the first recorded collision of an iceberg and a ship in Hudson Strait in 1686 (Hill 2000) icebergs have been a threat to shipping in the NW Atlantic. Records of scores of recorded collisions or sinkings every year exist from the late nineteenth century and early twentieth century (Hill 2000); it was only the foundation of the International Ice Patrol (IIP) following the tragic sinking of the RMS *Titanic* in 1912

that led to rapid reduction of the loss of life and vessels from iceberg collisions (Murphy & Cass 2012). However, the iceberg risk remains (Figure 1), and in recent decades iceberg numbers have tended to increase (Bigg et al. 2014), meaning the background risk has increased even though monitoring has improved (Christensen & Luzader 2012). This risk varies dramatically from one year to the next (Figure 2a) and even though the peak iceberg season is restricted to March to August (Figure 2b) icebergs have occurred in the shipping lanes east of Newfoundland and the Grand Banks in any month of the year.

The immediate iceberg risk is managed through the issuing of daily iceberg charts and bulletins (<https://www.navcen.uscg.gov/?pageName=iipCharts>) by the North American Ice Service, using information from the IIP, as well as weekly outlooks during the peak iceberg season. This effectively manages the short-term risk, as it is claimed that no vessel that has heeded IIP warnings has struck an iceberg (Murphy & Cass 2012). However, there is no correlation from one year to the next of the severity of the iceberg season, and no iceberg warnings are issued for timescales beyond the peak season weekly outlook. Nevertheless, longer term outlooks have the potential to significantly affect planning of marine operations and use and locations of principal North Atlantic shipping routes months in advance, as well as assisting with advance planning of the monitoring activities of the IIP and national coastguards.

In order to be able to produce seasonal forecasts of iceberg numbers it is first necessary to understand the root causes of the extreme annual variation in iceberg numbers seen in the Labrador Current, as represented by the number of icebergs larger than growler size crossing the 48°N parallel (henceforth called I48N). This has been attempted by both ocean-iceberg modelling (Bigg et al. 2014; Wilton et al. 2015) and a Windowed Error Reduction Ratio (WERR) control systems identification model

approach (Bigg et al., 2014; Zhao et al. 2016). The first approach used a general circulation model with an iceberg module to study the ocean circulation and iceberg trajectories and melting forced by observed climate variability over the whole of the twentieth century.

The second approach involved producing an optimised polynomial regression model for I48N forced by a range of environmental factors. Through this second approach, it was found that I48N is a complex, non-linear, lagged, function of three key large-scale environmental variables modulating the combined production, trajectory and melt rate of icebergs. The iceberg supply is represented by the changing surface mass balance of the Greenland Ice Sheet (GrIS), an ocean ice melting factor off Greenland is represented by the sea surface temperature of the Labrador Sea, and the atmospheric state of the North Atlantic, is epitomised by the North Atlantic Oscillation (Zhao et al., 2016).

Both approaches have demonstrated a strong link between a reconstructed flux of icebergs, originating largely from west and south Greenland (Wilton et al., 2015), and I48N of the following 1-3 years, with the ocean-iceberg modelling reproducing the I48N annual variation over 1900-2008 with a correlation of 0.83 and the WERR model with a correlation of 0.84 (Bigg et al., 2014). Most icebergs reaching 48°N, and so contributing to the spring peak in I48N, are shown by both methods to have calved from Greenland during the previous summer or autumn. Typically, the icebergs will have been frozen into the winter sea-ice between Baffin Bay and the Labrador coast, and the spring surge is due to their release during sea-ice melting. However, a minority of icebergs will have travelled a much longer path within Baffin Bay, taking up to another 2 years to reach 48°N (Wilton et al., 2015; Figure 1). The time lag between changes in these forcing variables, the response of the GrIS' iceberg calving and the time it takes

for icebergs to reach Newfoundland means that there is potential to produce iceberg number forecasts months to seasons in advance. In this prediction study the WERR control systems model is employed, using monthly forcing data, to forecast I48N up to 8 months in advance. In section 2 the methodology, and the data used, are described, along with the two approaches trialled here. The results of the two WERR model predictions are then validated in section 3 over the 20 year period 1997-2016, with the most successful case then being used in section 4 to predict the 2017 and 2018 fluxes. Note that at the time of preparation of the initial report of this study, provided to the IIP and North American Ice Service through the auspices of the Glacial Ice Hazard Working Group in December 2017, the 2017 values of I48N were not published. Both 2017 and 2018 are therefore trial predictions. The final section, 5, provides a summary and considers future developments for both the WERR approach to forecasting iceberg hazard and more spatially variable possibilities through ocean-iceberg modelling.

2. Data and Methodology

2.1 Data

Bigg et al. (2014) showed that I48N could be represented by a WERR model using the large-scale atmospheric, oceanic and glaciological measures of the North Atlantic Oscillation (NAO), mean Labrador Sea Surface Temperature (LSST) and Greenland Ice Sheet Surface Mass Balance (SMB) respectively. In this study monthly data were used. The monthly NAO time-series is the principal component-based version of this atmospheric circulation index (Hurrell and Deser (2009); <https://climatedataguide.ucar.edu/climate-data/hurrell-north-atlantic-oscillation-nao-index-pc-based>). By the nature of the principal component calculation technique, the individual monthly values change slightly every time the online dataset is extended, meaning the values used here from the 1900-2018 dataset are slightly different to those

used over 1900-2008 in Zhao et al. (2016). The Greenland SMB model calculation is described in Hanna et al. (2011), and is originally based on the runoff code of Janssens & Huybrechts (2000) with subsequent modification, but the values from 1997-2018 have been re-calculated/extended using the most recent ERA-Interim atmospheric reanalysis. The final input variable of the LSST comes from averaging the updated Kaplan v2 SST (Kaplan et al. 1998) over (67-55°N, 65-45°W). The Kaplan v2 SST is available from NOAA's Physical Sciences Division (<http://www.esrl.noaa.gov/psd>).

The I48N dataset itself has been, and continues to be, constructed by the IIP. The origin of the iceberg observations that lead to the I48N series has varied over the years. Originally, these were based on visual observations by ships of opportunity, but increasingly from 1913 onwards from dedicated ice detection vessels, and since the 1940s, aircraft. Now radar, satellite imagery and short-term iceberg drift modelling supplements such traditional observations, which are still reported (Christensen & Luzader 2012). While the accuracy of this dataset has no doubt increased over time, as detection methods have improved, the importance of knowing the iceberg risk means that even the early data are likely to be reasonably robust (Wilton et al., 2015). The monthly number of icebergs crossing 48°N over 1900-2011 is available in Table form at http://www.navcen.uscg.gov/pdf/iip/International_Ice_Patrols_Iceberg_Counts_1900_to_2011.pdf. Extensions of the monthly data up to September 2017 are contained within the IIP Annual Reports, available at <https://www.navcen.uscg.gov/?pageName=IIPAnnualReports>. The eastern limit of the line used is ~ 40°W (see IIP 2017). For the purposes of the iceberg count, only pieces of floating glacier ice greater than 5m in size are counted, and the Ice Year extends from October of the previous calendar year up to September of the nominal calendar year. Thus the 2017 Ice Year extended from October 2016 until September 2017. Note that

the verification study of this work was carried out using the Ice Years 1977-2016 (Figure 2) as at the time of analysis the 2017 Ice Year data were not yet available.

2.2 WERR methodology

While the full mathematical details of the WERR method are discussed in Zhao et al. (2016; 2017) it is worth summarising the approach here. The WERR system identification model uses a forward regression orthogonal least squares algorithm to build models term by term from recorded datasets. The WERR method searches through an initial library of polynomial model terms, which here includes linear and quadratic lagged variables, and selects the most significant terms to include in the final model. This selection is achieved by using the error reduction ratio (ERR_i) which shows the contribution that each polynomial model term, p_i , makes to the variance of the dependent variable (I48N here) expressed as a percentage:

$$ERR_i = \frac{g_i^2 \sum_{k=1}^L p_i^2(k)}{\sum_{k=1}^L I48N^2(k)} \quad (1)$$

where L is the window length, in months or years, and

$$g_i = \frac{\sum_{k=1}^L p_i(k)I48N(k)}{\sum_{k=1}^L I48N^2(k)} \quad (2)$$

ERR_i can vary from 0 to 1. The number of potential terms whose contribution needs to be checked at each step in the model creation depends on the polynomial order (here up to 2) and the number of lags allowed. If lags out to 48 months (49 linear terms for each input including the zero lag) are considered then there are 11026 candidate model terms for each temporal window, which includes 1 constant term, $49 \times 3 = 147$ first order or linear terms, and $(147+1) \times 147/2 = 10878$ second order terms. Details can be found in Eq. (9) in Zhao et al. (2017).

For this work, all terms with an $ERR_i > 0.01$ were retained, which happens to lead to models with uniformly 15 terms. All the models produced through the scenarios

discussed below are shown in Table A1. The WERR method allows the links between I48N and the forcing variables to evolve over time using a 30-year sliding window. The window is moved through the data, so that each window's model is created from the data of that particular 30-year window. Time variation in the balance of the environmental forcing characteristics will therefore be tracked using this approach. This includes effects that are longer than the window length as these longer term changes will moderate the data through this and neighbouring windows in a way that the sliding window approach can track. A visual representation of the fit of the model to I48N over the long term is shown in Figure 3.

2.3 Prediction methodology

Monthly data for the three forcing variables of the NAO, LSST and SMB were gathered or calculated up to January 2018 for our prediction attempt using the WERR method. Previous work had suggested that the dominant terms in the WERR model of recent decades had a lag of 8 months or longer (Zhao et al. 2016; Marsh et al. 2017), linked to the minimum time it takes for an iceberg to travel from the closest calving site in southern Greenland to the Newfoundland coast south of 48°N. A prediction of the I48N numbers up to September 2018, that is the close of the 2018 Ice Year, was therefore attempted. The WERR model developed for Marsh et al. (2017) was extended up to 2016 in this analysis. To provide an ensemble of possible models to test the reproducibility of our prediction method, we took the sliding window models for the 11 periods of 1977-2006 up to 1987-2016 to form our ensemble. This allows us to seek the impact of the evolution of the model relationship between I48N and the forcing variables on our prediction. This model evolution is normally slight; for example, the first model term is a quadratic in NAO with a lag of 15 months for each member of the ensemble (see Table A1).

The previous research using the WERR approach was fitting models to a known variation in I48N. Therefore all lags from 0 months up to a maximum of 48 months were in the library of model terms from which the optimization scheme was selected. In attempting to predict the NW Atlantic ice hazard well in advance, only terms with a lag of the prediction time or longer could be used in the model construction, potentially downgrading the model's accuracy through exclusion of terms involving variables with no or small time lags. Thus, here two cases were tested:

- *Case A*: models allowing the full range of lag terms were calculated, but only those terms in the model were included in the prediction test used here that had an ERR contribution above that of the first full model term containing a lag term of 7 months or less. This restricted the number of model terms to between 1 and 6, depending on the ensemble member. The bold terms in Table A1 shows how the Case A model order changes across the sliding windows.
- *Case B*: WERR models were developed using a restricted set of initial library terms for model selection, so that only terms with a lag of 8 months or longer were permitted. To save on computation, those final model terms contributing less than 0.02 to ERR were excluded. This means the ensemble models contained between 6 and 9 terms, rather than the full 15, depending on the ensemble member; these are shown in bold in Table A1.

The ensemble model terms used for both Case A and B tests are given in Table A1. The test case models' outcome was verified through a comparison of the predictions of the two cases and the actual I48N numbers over the twenty (Ice) years of 1997-2016. Results from both Cases are presented here, but it will be shown that those

for Case B match much better in the verification period and so it is the Case B test prediction that is used for the formal prediction of I48N in 2017 and 2018.

3. Verification Results

It is worth noting that while the models give monthly predictions and the evolution of the annual cycle is reproduced by the models, in terms of the slow increase in the late winter and early spring, maximum increase in spring to early summer, and a declining contribution to I48N during the late summer and autumn, cumulative measures are more robustly predicted. This study's verification for Cases A and B therefore concentrates on the cumulative values of I48N over the onset period of January-May and the main season of January-September. The results of the predictions for 2017 and 2018 iceberg seasons will, however, show the full set of monthly predictions.

3.1 Case A

For Case A the model predictions for the verification period of 1997-2016 are shown in Table 1. Table 1 shows a considerable difference in the mean I48N predictions compared to the observed values for both the onset and main season numbers, with the predictions substantially under-estimating the observed means. As the standard deviation of the observations over the period is large, there is no statistically significant difference between the observed and predicted sets of means for May or September respectively. The distributions of both sets of data are, however, bi-modal (Figure 4), although the observed I48N has more pronounced extremes than either model's prediction.

While it is clear that the Case A model would be a poor estimate of the actual I48N numbers it may be that the similarity of the distributions means that categorisation of the predicted level of the iceberg numbers might be feasible. The bi-modal nature of the observed I48N suggests it would be of value to be able to forecast a "low" or "high"

iceberg number season. The set of I48N observations and predictions in Table 1 were therefore categorised into low or high values, depending on whether they were below or above the mean values for the 20-year verification period of the respective variables given in Table 1. This ranking is shown in Table 2.

In Table 2, 13 of the 20 years of observations and predictions show the same categorisation for May and 14 for September. Using the Sign test (Huntsberger and Billingsley 1973) the latter shows a statistically significant compatibility of categorisation at the 5% level. Nevertheless, the correlation of the September I48N observations and predictions for the verification period is only 0.43, slightly below the 0.44 level required for statistical significance at the 5% level. The May relationships for both correlation (0.34) and the sign test (7.4%) are not significant. Therefore, while there is some evidence that main season categorisation for Case A models is possible, the evidence is not statistically strong enough to be confident in making a forecast using this approach.

3.2 Case B

The Case B models involve a reduced set of model terms that can contribute to the WERR model, with only those having lags of 8 months or greater being permitted to be in the term library from which the model selects its terms for a given 30-year sliding window. Such an approach allows seasonal forecasting to be a reality, but may mean the resulting models are less accurate than the full term models used in previous studies such as Zhao et al. (2016). The results of the verification study for Case B in comparing the mean predictions of the onset and prediction periods for 1997-2016 are shown in Table 3.

In contrast to the situation for Case A, Table 3 shows similar means for both the May, and, especially, the September values between the observed and forecast I48N. As

for Case A, the WERR model under-estimates the degree of interannual variability, and also is unsuccessful in reproducing the extreme highs and lows of the 1997-2016 period. However, the base level mean similarity gives promise for estimation of the relative level of iceberg numbers for a given year. The distributions of the observed and predicted I48N over the verification period are also similar, with a bi-modal pattern shown in Figure 4c. The similarities of the means and distributions, particularly the fact that both observations and Case B predictions have their secondary peak a little below 1000 icebergs a year, suggest a categorisation approach may be useful for prediction of the iceberg hazard level. The set of I48N observations and predictions in Table 3 were therefore categorised into low or high values, depending on whether they were below or above the mean values for the 20-year verification period of the respective variables given in Table 2. This ranking is shown in Table 4.

In Table 4, 16 of the 20 years (80%) show the same categorisation for both May and September. This is rather more than was the situation for Case A, and using the Sign test shows a statistically significant compatibility of categorisation for both periods at the 0.5% level. The correlation of the I48N observations and Case B predictions for the verification period are also high, at 0.64 for accumulated values from January to May and 0.60 for January to September respectively; these are statistically significant at the 1% level.

The statistical robustness of the Case B verification suggests that we can examine the details of the 2017 and 2018 predictions with a confidence of 80% that the predictions are robust. In the next section we will examine these predictions using the Case B WERR modelling approach.

4. Case B Predictions

The new version of the WERR model, Case B, where only terms with lags of 8 months or longer are used in constructing the predictive model has been shown in section 3.2 to be robust in its ability to hindcast the observed I48N numbers during the onset and main iceberg seasons. The monthly predictions for the 2017 and 2018 seasons are shown in Table 5. While the predicted individual monthly accumulation rates are lower than the observations from March onwards (Table 5 and Figure 5), each month's predicted iceberg numbers for 2017 and 2018 are all above average predictions (Table 3), and average observations, for the 1997-2016 period. This is particularly true of the 2017 hindcast; 2018, while the monthly predictions are above the 20-year mean of predictions, and observations, for all months, has a lower I48N prediction for the season as a whole than 2017 by almost 100 icebergs. Note that the 2017 Ice year was unusual in that there was an earlier eruption of icebergs from the sea-ice zone than normal (Figure 4), due to break-up of High Arctic sea-ice structures and their purging through Baffin Bay and the Labrador Current this year (Barber et al. 2018). This may well have carried more icebergs than expected from Baffin Bay into the Labrador Sea, making a closer model fit unlikely. Nevertheless, the 2017 prediction was still within the error bars of the observed I48N.

Information about the predictions that we haven't yet used, however, comes from the range of the ensemble members which led to the standard deviations of the predictions in Table 5. The values for the 11 ensemble members for May and September 2017 and 2018 are given in Table 6. Two things are notable about this table. Firstly, all of the four predictions show a majority (either seven (64%) or eight (73%) of eleven) of ensemble members lie above the long term mean of the Case B verification study. Secondly, almost all of the lower ensemble members are in the first three ensemble models. The later ensembles, which have come from sliding window models formed

from data closer to the prediction dates, are strongly consistent with a higher than normal I48N. Both of these facts add confidence to the 2017 and 2018 predictions of high iceberg numbers being robust, but of 2018's I48N level being 10-20% below that of 2017.

A further feature comes from examination of the details of the Case B verification. The standard deviation of the predictions is only around half that of the observations, with the extreme highs and lows of the observed I48N series poorly reproduced in particular. This property is discussed further in section 5. However, four of the five years shown in Table 3 where the observed I48N in September was above 1000 led to hindcast values above those given for the 2017 and 2018 September predictions. In addition, for each of the three years in Table 3 where the May observed I48N was above 1000 the hindcast values are above those predicted for 2017 and 2018. It therefore seems likely that the higher I48N values predicted for 2017 and 2018 will be at the lower end of the upper peak, around or below 1000. This indeed was the case for 2017, where the observed I48N for the year was 1008.

5. Discussion and Conclusion

The above analysis shows that the Case B WERR model approach is very likely to lead to a sound prediction of whether an iceberg year will be a low or high number season. For both 2017 and 2018 the model predicted a high iceberg number season, with an 80% skill record from the 1997-2016 verification period. From the verification analysis, the confidence in the high iceberg number prediction is 71%, although this may be an under-estimate due to the increased reliability of the later ensemble members.

Indications from the analysis are also that the predicted high iceberg numbers are likely NOT to be at the extreme end of the spectrum, and so ≤ 1000 across the full season, with 2018's I48N being $\sim 10\%$ lower than 2017's.

Of the two ways of using the WERR method to produce predictions Case B has been shown to be much more robust than Case A. Having a time lag of 8 months in the terms available for the model construction decreases the correlation of I48N hindcasts and observations from 0.84, when using terms with all lags (Bigg et al. 2014), to 0.60-0.64. However, this does not materially compromise the ability of the WERR model to reproduce the I48N time series as the correlation is still statistically significant at the 1% level.

This time lag of 8 months was chosen as it was a dominant lag in the full model when used across the twentieth century (Zhao et al. 2016), largely because this timescale stems from the minimum time it takes for icebergs to drift from calving sites in the southwestern quadrant of Greenland to the shipping lanes off southern Newfoundland (Wilton et al. 2015). The fact that the correlation of the verification hindcasts with I48N observations remains highly statistically significant using the Case B model, with only 8-month or longer lags, demonstrates that the main cause of the interannual I48N fluctuation stems from changes over and around Greenland and not from the variation in the oceanic and atmospheric conditions affecting the icebergs en route. This conclusion was separately reached previously through an ocean modelling study (Bigg et al. 2014). While the high standard deviation of the observed I48N is likely to be due to the vagaries of the conditions experienced by the icebergs while drifting south, something not captured by either the Case A or B predictions (Tables 1 and 3), but more visible in the longer term full model comparison of Figure 3, the underlying year-to-year peaks and troughs in calving are captured reasonably well by the Case B predictions. From the model equations, shown in Table A1, the main effects leading to the hindcast variability are driven by the climate in the winter and spring of the preceding year over Greenland, as seen through the NAO, but in convolution with

ocean temperatures (the LSST), linked to calving tendency, and the Greenland surface mass balance (SMB), in terms of the weighting of short-term melting and precipitation.

The time lag of 8 months also allows a useful level of advance notice for shipping, monitoring and policy responses to forecasts of the next Labrador ice season. Data from no later than September are required for forecasts of the onset and peak iceberg season up to May in the following year. Data for a full forecast of the whole season until September are needed from no later than January. Some of the fields are not compiled and generally released for another couple of months, but this still allows the possibility of a pre-Christmas forecast for the main part of the next ice season up to May. This was achieved for this study, and advanced notice given to relevant ice hazard monitoring schemes.

This study is just a beginning to addressing the need for seasonal forecasts of the ice hazard in the NW Atlantic. For example, it is feasible to gather the required data on the key forcing fields of SMB, NAO and LSST much earlier, with at most a month's delay. Discussions are already underway with key agencies to achieve this ideal. There is also excellent potential to adapt the model for specific purposes. Forecast warning time could be lengthened through using terms with longer lags. The forecasts could be used as input to ocean-iceberg models, forced by atmospheric forecast fields, to provide forecast iceberg density maps as well as the bulk estimate made here. Indeed, this has already been trialled in a hindcast study (Marsh et al. 2017). These various options will be investigated in future work.

The two forecasts so far calculated also offer promise for the future. The 2017 forecast predicted a high iceberg season, with likely iceberg numbers crossing 48°N by the end of the season of around 1000. The observed number of 1008 fitted this well, and indeed while the method tends to under-estimate the actual numbers seen during high

Ice years, on this occasion the observed number fell within the error bounds of the prediction (766 ± 297). The 2018 forecast is for a relatively high iceberg season, but at a lower level than in 2017. As of the time of writing (early April), it was clear that 2018 was indeed going to be a year with lower iceberg numbers than 2017. By 30th March, around the beginning of the peak iceberg season in 2017 there were already 319 icebergs south of 50°N, while in 2018 this number was reduced to 72 (<https://www.navcen.uscg.gov/?pageName=iipCharts&Archives>). Similarly, by 30th June only 9 icebergs remained south of 48°N in 2018, while 29 were present at the same date in 2017. There was also no sign upstream in 2018 of the large iceberg armada moving south that was seen accompanying the High Arctic sea-ice purge of 2017 (Barber et al. 2018). It is planned to make the 2019 forecast generally available late in 2018.

Appendix

Table A1. WERR Models. All terms are shown, but only those in **BOLD** were used for the Case A and Case B models. Columns: Rank – order of selection of term in model; Term – linear or quadratic term in variables NAO, LSST or SMB (see main text for definition), with lags, in x months, given by “(t-x)”; ERR – error reduction achieved by term; Coefficient – multiplying factor for term. As an example of model structure, the CASE A model for the sliding window January 1983 to December 2012 is given by $I48N = 20.43557.NAO(t-15).NAO(t-15) + 66.67288.NAO(t-15).LSST(t-15)$

Case A - Without prediction constraint				Case B - With 8 months prediction constraint			
1977-Jan to 2006-Dec				1977-Jan to 2006-Dec			
Rank	Term	ERR	Coefficient	Rank	Term	ERR	Coefficient
1	NAO(t-15)*NAO(t-15)	0.37006	20.93348	1	NAO(t-15)*NAO(t-15)	0.37006	12.0422
2	LSST(t-9)	0.07709	-129.33035	2	LSST(t-9)	0.07709	-146.91238
3	SMB(t-46)*SMB(t-46)	0.0638	0.01424	3	SMB(t-46)*SMB(t-46)	0.0638	0.01436
4	SMB(t-45)*LSST(t-9)	0.04234	1.91529	4	SMB(t-45)*LSST(t-9)	0.04234	2.08521
5	SMB(t-45)*SMB(t-46)	0.03922	-0.02291	5	SMB(t-45)*SMB(t-46)	0.03922	-0.01544
6	NAO(t-6)*NAO(t-29)	0.03666	19.20371	6	NAO(t-17)*NAO(t-29)	0.02759	16.43892
7	SMB(t-29)*NAO(t-3)	0.01989	0.4972	7	SMB(t-47)*LSST(t-11)	0.02126	0.75765
8	NAO(t-17)*NAO(t-29)	0.02121	13.93881	8	NAO(t-28)*NAO(t-29)	0.01818	13.76663
9	SMB(t-17)*SMB(t-29)	0.01678	0.00876	9	NAO(t-28)*LSST(t-18)	0.0161	38.14445
10	NAO(t-15)*NAO(t-41)	0.017	19.25682	10	SMB(t-29)*SMB(t-29)	0.01601	0.00934
11	SMB(t-33)*NAO(t-1)	0.01566	0.40561	11	NAO(t-15)*NAO(t-41)	0.01375	18.99633
12	SMB(t-47)*NAO(t-39)	0.01245	0.3607	12	NAO(t-29)*NAO(t-38)	0.0129	-17.95814
13	SMB(t-18)*NAO(t-39)	0.01155	0.32684	13	SMB(t-11)*NAO(t-38)	0.01485	0.35524

14	SMB(t-35)*LSST(t-20)	0.0121	0.70334	14	SMB(t-13)*SMB(t-29)	0.01046	0.00884
15	NAO(t-7)*NAO(t-14)	0.01001	-19.44967	15	SMB(t-46)*NAO(t-15)	0.00992	-0.38047

1978-Jan to 2007-Dec				1978-Jan to 2007-Dec			
1	NAO(t-15)*NAO(t-15)	0.37471	23.06877	1	NAO(t-15)*NAO(t-15)	0.37471	18.70263
2	LSST(t-9)	0.07493	-77.68674	2	LSST(t-9)	0.07493	-93.32273
3	LSST(t-8)*LSST(t-9)	0.05899	65.25206	3	LSST(t-8)*LSST(t-9)	0.05899	74.10143
4	NAO(t-28)*NAO(t-29)	0.04456	15.01338	4	NAO(t-28)*NAO(t-29)	0.04456	13.89635
5	NAO(t-15)*NAO(t-39)	0.03279	10.85672	5	NAO(t-15)*NAO(t-39)	0.03279	17.65898
6	SMB(t-29)*NAO(t-27)	0.02296	0.31409	6	SMB(t-29)*NAO(t-27)	0.02296	0.28172
7	NAO(t-7)*NAO(t-15)	0.02054	-24.98646	7	SMB(t-35)*NAO(t-38)	0.01918	0.51271
8	SMB(t-5)*NAO(t-2)	0.0244	0.41842	8	SMB(t-8)*SMB(t-46)	0.01858	-0.01499
9	NAO(t-39)*NAO(t-47)	0.01748	17.74942	9	NAO(t-17)*NAO(t-29)	0.01876	20.53809
10	NAO(t-16)*LSST(t-24)	0.01431	-33.95906	10	NAO(t-15)*NAO(t-41)	0.01937	19.87054
11	NAO(t-1)*NAO(t-36)	0.01415	13.92174	11	SMB(t-21)*SMB(t-21)	0.01642	0.00625
12	SMB(t-6)*NAO(t-39)	0.01425	0.39402	12	NAO(t-14)*LSST(t-43)	0.01192	-30.36313
13	NAO(t-15)*LSST(t-15)	0.01345	36.00799	13	SMB(t-21)*LSST(t-9)	0.01177	0.90358
14	SMB(t-46)*SMB(t-46)	0.01317	0.00629	14	NAO(t-40)*NAO(t-46)	0.01235	-24.4327
15	SMB(t-35)*NAO(t-38)	0.01358	0.41987	15	SMB(t-20)*NAO(t-41)	0.01231	0.32464

1979-Jan to 2008-Dec				1979-Jan to 2008-Dec			
1	NAO(t-15)*NAO(t-15)	0.36292	20.70761	1	NAO(t-15)*NAO(t-15)	0.36292	22.54386
2	LSST(t-9)	0.06819	-72.16229	2	LSST(t-9)	0.06819	-70.76018
3	LSST(t-8)*LSST(t-9)	0.05564	92.873	3	LSST(t-8)*LSST(t-9)	0.05564	80.73332
4	NAO(t-28)*NAO(t-29)	0.03827	18.32166	4	NAO(t-28)*NAO(t-29)	0.03827	14.7938
5	NAO(t-15)*NAO(t-39)	0.03215	12.71244	5	NAO(t-15)*NAO(t-39)	0.03215	13.46352
6	SMB(t-5)*LSST(t-13)	0.02653	1.01055	6	SMB(t-9)*SMB(t-21)	0.02603	0.01171
7	NAO(t-40)*LSST(t-38)	0.02534	42.66617	7	SMB(t-8)*SMB(t-46)	0.0353	-0.01422
8	NAO(t-17)*NAO(t-29)	0.01972	16.3628	8	NAO(t-40)*LSST(t-38)	0.01844	44.47945

9	SMB(t-42)*NAO(t-27)	0.01773	0.36978	9	SMB(t-35)*NAO(t-38)	0.01536	0.54795
10	SMB(t-5)*NAO(t-2)	0.01794	0.42122	10	NAO(t-15)*LSST(t-15)	0.01609	28.32399
11	NAO(t-39)*NAO(t-47)	0.01759	24.25575	11	NAO(t-14)*NAO(t-47)	0.01414	14.75576
12	NAO(t-1)*NAO(t-36)	0.01251	11.06214	12	SMB(t-35)*NAO(t-14)	0.01377	-0.56135
13	NAO(t-16)*NAO(t-40)	0.01201	16.45818	13	NAO(t-14)*LSST(t-41)	0.01414	-37.87206
14	SMB(t-44)*NAO(t-40)	0.01171	-0.39749	14	NAO(t-17)*NAO(t-29)	0.013	13.62479
15	NAO(t-14)*NAO(t-47)	0.01259	16.8937	15	SMB(t-9)*NAO(t-35)	0.01145	0.40612

1980-Jan to 2009-Dec				1980-Jan to 2009-Dec			
1	NAO(t-15)*NAO(t-15)	0.36127	20.31486	1	NAO(t-15)*NAO(t-15)	0.36127	20.05216
2	NAO(t-6)*NAO(t-29)	0.06121	22.76674	2	NAO(t-28)*NAO(t-28)	0.06116	9.24127
3	SMB(t-7)*NAO(t-15)	0.04502	0.3972	3	LSST(t-9)	0.05229	-72.82291
4	NAO(t-28)*NAO(t-28)	0.04616	10.93291	4	LSST(t-8)*LSST(t-9)	0.03991	89.56479
5	SMB(t-8)*SMB(t-46)	0.03532	-0.01601	5	SMB(t-8)*SMB(t-46)	0.03371	-0.0175
6	LSST(t-8)*LSST(t-9)	0.03633	99.93176	6	SMB(t-9)*SMB(t-21)	0.0483	0.01255
7	NAO(t-15)*LSST(t-13)	0.02997	35.667	7	NAO(t-15)*LSST(t-14)	0.02701	29.19803
8	NAO(t-40)*LSST(t-38)	0.02712	45.95632	8	NAO(t-40)*LSST(t-38)	0.02608	39.73453
9	SMB(t-9)*SMB(t-21)	0.02393	0.01018	9	NAO(t-17)*NAO(t-29)	0.01626	16.87268
10	LSST(t-8)	0.02353	-45.358	10	SMB(t-35)*NAO(t-38)	0.01357	0.43758
11	LSST(t-6)*LSST(t-11)	0.0172	-104.16038	11	NAO(t-14)*LSST(t-41)	0.01363	-44.02547
12	NAO(t-7)*NAO(t-14)	0.0144	-26.74154	12	SMB(t-35)*NAO(t-14)	0.02171	-0.56654
13	NAO(t-1)*NAO(t-36)	0.01414	13.37672	13	LSST(t-21)*LSST(t-28)	0.01304	-62.2622
14	NAO(t-2)*NAO(t-28)	0.013	15.11862	14	SMB(t-20)*NAO(t-41)	0.01225	0.3938
15	SMB(t-9)*NAO(t-2)	0.01065	-0.30051	15	SMB(t-33)*NAO(t-40)	0.01305	-0.3572

1981-Jan to 2010-Dec				1981-Jan to 2010-Dec			
1	NAO(t-15)*NAO(t-15)	0.35175	23.09162	1	NAO(t-15)*NAO(t-15)	0.35175	22.48843
2	NAO(t-28)*NAO(t-29)	0.06108	15.77621	2	NAO(t-28)*NAO(t-29)	0.06108	15.24083
3	NAO(t-39)*NAO(t-39)	0.05227	12.65222	3	NAO(t-39)*NAO(t-39)	0.05227	15.07007

4	SMB(t-5)*NAO(t-2)	0.03684	0.52466	4	NAO(t-15)*NAO(t-16)	0.03661	18.08788
5	NAO(t-17)*NAO(t-29)	0.03444	15.89582	5	NAO(t-15)*NAO(t-47)	0.03002	22.31135
6	SMB(t-40)*NAO(t-27)	0.02724	0.49748	6	SMB(t-40)*NAO(t-27)	0.02655	0.62498
7	NAO(t-25)*NAO(t-28)	0.03148	28.00612	7	NAO(t-25)*NAO(t-28)	0.02787	23.96898
8	SMB(t-9)*LSST(t-9)	0.02481	-1.05381	8	SMB(t-9)*LSST(t-21)	0.02465	-1.02514
9	SMB(t-8)*NAO(t-13)	0.02275	-0.35574	9	SMB(t-8)*NAO(t-13)	0.02535	-0.50573
10	SMB(t-46)*SMB(t-46)	0.01886	0.00771	10	SMB(t-46)*SMB(t-46)	0.01922	0.00887
11	NAO(t-7)*NAO(t-14)	0.022	-21.61194	11	NAO(t-15)*LSST(t-13)	0.01604	39.84936
12	SMB(t-26)*NAO(t-15)	0.01691	1.26295	12	NAO(t-37)*LSST(t-9)	0.01423	-26.86158
13	SMB(t-14)*NAO(t-15)	0.02393	-1.13449	13	NAO(t-26)*NAO(t-29)	0.01223	18.05206
14	NAO(t-16)*LSST(t-37)	0.01297	31.68283	14	SMB(t-44)*NAO(t-27)	0.01233	-0.3173
15	NAO(t-36)*LSST(t-43)	0.01286	-26.41269	15	SMB(t-8)*SMB(t-31)	0.01185	-0.00703

1982-Jan to 2011-Dec				1982-Jan to 2011-Dec			
1	NAO(t-15)*NAO(t-15)	0.27508	17.48852	1	NAO(t-15)*NAO(t-15)	0.27508	13.92661
2	NAO(t-15)*LSST(t-4)	0.09587	45.2272	2	SMB(t-29)*NAO(t-15)	0.09331	0.44737
3	NAO(t-39)*NAO(t-39)	0.05999	9.84542	3	NAO(t-28)*NAO(t-28)	0.06794	15.03671
4	NAO(t-6)*NAO(t-29)	0.05804	19.3779	4	SMB(t-8)*SMB(t-46)	0.04255	-0.01963
5	NAO(t-2)	0.04354	21.78788	5	SMB(t-9)*SMB(t-9)	0.03728	0.00635
6	SMB(t-40)*NAO(t-27)	0.03621	0.48114	6	NAO(t-17)*NAO(t-29)	0.03936	18.49671
7	NAO(t-25)*NAO(t-28)	0.03189	17.29264	7	NAO(t-15)*NAO(t-41)	0.0275	29.05513
8	SMB(t-8)*SMB(t-46)	0.01777	-0.01232	8	SMB(t-31)*SMB(t-35)	0.02058	0.00956
9	SMB(t-9)*SMB(t-21)	0.03241	0.00873	9	NAO(t-28)*NAO(t-34)	0.01747	27.8608
10	SMB(t-46)*NAO(t-15)	0.01969	-0.39114	10	NAO(t-37)*LSST(t-43)	0.01744	-31.56919
11	NAO(t-28)*NAO(t-30)	0.01807	18.31393	11	SMB(t-9)*NAO(t-25)	0.01639	0.35875
12	NAO(t-15)*NAO(t-47)	0.01497	20.0062	12	NAO(t-39)*LSST(t-16)	0.01723	32.54011
13	NAO(t-1)*NAO(t-36)	0.016	13.6655	13	NAO(t-39)*LSST(t-8)	0.01654	-43.98501
14	SMB(t-9)*NAO(t-2)	0.01569	-0.28269	14	SMB(t-24)*NAO(t-27)	0.01647	0.39752
15	NAO(t-16)*NAO(t-27)	0.01497	14.83183	15	NAO(t-15)*NAO(t-16)	0.01474	12.61278

1983-Jan to 2012-Dec				1983-Jan to 2012-Dec			
1	NAO(t-15)*NAO(t-15)	0.25965	20.43557	1	NAO(t-15)*NAO(t-15)	0.25965	23.22433
2	NAO(t-15)*LSST(t-15)	0.10281	66.67288	2	NAO(t-15)*LSST(t-15)	0.10281	56.57531
3	NAO(t-6)*NAO(t-29)	0.06478	27.19264	3	NAO(t-28)*NAO(t-28)	0.06036	7.75748
4	NAO(t-27)*NAO(t-27)	0.05715	3.79551	4	SMB(t-8)*SMB(t-46)	0.04467	-0.01339
5	NAO(t-2)	0.03752	20.50279	5	SMB(t-9)*SMB(t-9)	0.04717	0.00704
6	SMB(t-40)*NAO(t-39)	0.03781	0.46651	6	NAO(t-17)*NAO(t-29)	0.03505	18.43852
7	NAO(t-40)*LSST(t-38)	0.02816	51.85951	7	SMB(t-15)*NAO(t-27)	0.02649	0.45616
8	NAO(t-28)*NAO(t-28)	0.02364	11.75895	8	LSST(t-8)*LSST(t-13)	0.02242	-51.99037
9	SMB(t-8)*SMB(t-46)	0.02357	-0.01184	9	SMB(t-35)*LSST(t-19)	0.01928	1.3139
10	SMB(t-9)*SMB(t-9)	0.03012	0.00573	10	SMB(t-35)*LSST(t-31)	0.01995	-1.07768
11	NAO(t-38)*LSST(t-41)	0.01607	-36.36013	11	NAO(t-39)*NAO(t-47)	0.01926	23.17552
12	NAO(t-1)*NAO(t-36)	0.01807	14.71473	12	SMB(t-31)*NAO(t-39)	0.01653	0.2898
13	SMB(t-9)*NAO(t-2)	0.01813	-0.314	13	SMB(t-23)*NAO(t-13)	0.01365	0.39849
14	SMB(t-47)*NAO(t-30)	0.01493	-0.28537	14	NAO(t-40)*LSST(t-38)	0.01545	35.97512
15	LSST(t-1)*LSST(t-21)	0.01336	-64.91018	15	NAO(t-15)*NAO(t-47)	0.01358	18.63497

1984-Jan to 2013-Dec				1984-Jan to 2013-Dec			
1	NAO(t-15)*NAO(t-15)	0.26073	20.72285	1	NAO(t-15)*NAO(t-15)	0.26073	18.8801
2	NAO(t-15)*LSST(t-15)	0.12472	52.2867	2	NAO(t-15)*LSST(t-15)	0.12472	51.77163
3	NAO(t-28)*NAO(t-28)	0.04867	13.64863	3	NAO(t-28)*NAO(t-28)	0.04867	5.97852
4	NAO(t-2)	0.04598	24.83485	4	NAO(t-40)*LSST(t-38)	0.04186	42.85402
5	NAO(t-39)	0.0393	23.92483	5	SMB(t-8)*SMB(t-46)	0.02943	-0.01435
6	NAO(t-6)*NAO(t-29)	0.0363	20.86001	6	SMB(t-9)*SMB(t-9)	0.03366	0.00722
7	NAO(t-28)*LSST(t)	0.02952	39.71928	7	NAO(t-39)*LSST(t-26)	0.02725	33.35643
8	SMB(t-8)*SMB(t-46)	0.02537	-0.0116	8	NAO(t-16)*NAO(t-29)	0.02344	17.05896
9	SMB(t-9)*SMB(t-9)	0.02357	0.00651	9	NAO(t-15)*NAO(t-41)	0.01945	20.78917
10	NAO(t-40)*LSST(t-38)	0.02523	41.02904	10	SMB(t-11)*NAO(t-38)	0.02181	0.45834

11	NAO(t-39)*NAO(t-47)	0.01837	20.3549	11	NAO(t-14)*NAO(t-47)	0.01994	19.0679
12	NAO(t-1)*NAO(t-36)	0.01787	11.80135	12	NAO(t-28)*NAO(t-34)	0.0173	24.64092
13	NAO(t-3)*NAO(t-4)	0.01485	-12.37561	13	LSST(t-19)*LSST(t-39)	0.01327	-79.55168
14	SMB(t-46)*NAO(t-15)	0.01378	-0.32901	14	NAO(t-29)*NAO(t-29)	0.01393	10.40664
15	NAO(t-15)*NAO(t-47)	0.01381	18.55772	15	NAO(t-16)*NAO(t-43)	0.01313	16.68583

1985-Jan to 2014-Dec				1985-Jan to 2014-Dec			
1	NAO(t-15)*NAO(t-15)	0.23536	22.7706	1	NAO(t-15)*NAO(t-15)	0.23536	26.22621
2	NAO(t-15)*LSST(t-15)	0.11772	67.08897	2	NAO(t-15)*LSST(t-15)	0.11772	57.48812
3	NAO(t-14)*LSST(t-44)	0.08303	-33.38563	3	NAO(t-14)*LSST(t-44)	0.08303	-44.64461
4	NAO(t-28)*NAO(t-28)	0.05376	21.14789	4	NAO(t-28)*NAO(t-28)	0.05376	13.7081
5	NAO(t-2)	0.03638	17.76066	5	SMB(t-21)*LSST(t-21)	0.03382	-0.91717
6	NAO(t-6)*NAO(t-29)	0.03255	19.97515	6	SMB(t-30)*NAO(t-27)	0.02698	0.45883
7	NAO(t-28)*LSST(t)	0.03335	38.12304	7	NAO(t-15)*NAO(t-41)	0.02258	21.51814
8	SMB(t-21)*LSST(t-40)	0.02398	-0.91069	8	SMB(t-35)*LSST(t-21)	0.02225	1.00672
9	NAO(t-39)*LSST(t-25)	0.02948	40.19181	9	SMB(t-8)*SMB(t-46)	0.0244	-0.00938
10	NAO(t-15)*NAO(t-41)	0.01873	15.57257	10	SMB(t-24)*NAO(t-27)	0.02232	0.37697
11	SMB(t-8)*SMB(t-46)	0.01848	-0.01104	11	NAO(t-25)*NAO(t-28)	0.01732	20.61168
12	SMB(t-21)*LSST(t-32)	0.01763	0.79948	12	SMB(t-8)*NAO(t-13)	0.01594	-0.29197
13	NAO(t-40)*LSST(t-26)	0.01362	35.99955	13	SMB(t-42)*LSST(t-38)	0.0128	0.84207
14	NAO(t-1)*NAO(t-36)	0.01363	11.70619	14	NAO(t-15)*NAO(t-47)	0.01381	20.0413
15	SMB(t-11)*NAO(t-30)	0.01231	-0.22588	15	LSST(t-29)*LSST(t-37)	0.01582	-64.35686

1986-Jan to 2015-Dec				1986-Jan to 2015-Dec			
1	NAO(t-15)*NAO(t-15)	0.23001	18.23097	1	NAO(t-15)*NAO(t-15)	0.23001	24.57823
2	NAO(t-15)*LSST(t-15)	0.11673	53.69955	2	NAO(t-15)*LSST(t-15)	0.11673	79.44829
3	NAO(t-14)*LSST(t-44)	0.07637	-29.77325	3	NAO(t-14)*LSST(t-44)	0.07637	-39.44514
4	SMB(t-21)*SMB(t-21)	0.05615	0.00699	4	SMB(t-21)*SMB(t-21)	0.05615	0.00648
5	NAO(t-25)*NAO(t-28)	0.04729	27.53758	5	NAO(t-25)*NAO(t-28)	0.04729	22.98647

6	SMB(t-8)*SMB(t-46)	0.04408	-0.01522	6	SMB(t-8)*SMB(t-46)	0.04408	-0.01472
7	NAO(t-3)	0.03501	25.38868	7	NAO(t-16)*LSST(t-21)	0.02465	-36.97192
8	NAO(t-16)*NAO(t-29)	0.03147	17.2743	8	NAO(t-15)*LSST(t-29)	0.02255	-44.99723
9	NAO(t-6)*NAO(t-29)	0.02097	18.57828	9	NAO(t-28)*NAO(t-29)	0.02514	22.9113
10	LSST(t-2)*LSST(t-35)	0.01893	-101.73501	10	SMB(t-9)*NAO(t-25)	0.02224	0.34153
11	SMB(t-40)*NAO(t-27)	0.01615	0.36957	11	SMB(t-42)*NAO(t-27)	0.01827	0.32732
12	SMB(t-9)*NAO(t-3)	0.01523	-0.38453	12	NAO(t-30)*NAO(t-39)	0.01294	-17.41382
13	Const.	0.01466	27.51333	13	NAO(t-14)*NAO(t-18)	0.01598	20.91167
14	NAO(t-1)*NAO(t-36)	0.01228	11.24793	14	NAO(t-15)*NAO(t-47)	0.00919	18.25769
15	NAO(t-28)*NAO(t-37)	0.00956	14.02879	15	SMB(t-44)*LSST(t-32)	0.01046	0.60053

1987-Jan to 2016-Dec				1987-Jan to 2016-Dec			
1	NAO(t-15)*NAO(t-15)	0.22126	25.23321	1	NAO(t-15)*NAO(t-15)	0.22126	28.83026
2	NAO(t-15)*LSST(t-15)	0.12799	60.07859	2	NAO(t-15)*LSST(t-15)	0.12799	76.26225
3	NAO(t-2)	0.07329	19.71261	3	NAO(t-14)*NAO(t-41)	0.06971	19.85428
4	SMB(t-21)*SMB(t-21)	0.06953	0.00797	4	SMB(t-21)*SMB(t-21)	0.05596	0.00747
5	SMB(t-8)*SMB(t-46)	0.05105	-0.01181	5	SMB(t-8)*SMB(t-46)	0.05079	-0.01328
6	NAO(t-25)*NAO(t-28)	0.03647	25.81293	6	NAO(t-25)*NAO(t-28)	0.03681	22.82284
7	NAO(t-6)*NAO(t-29)	0.03218	20.15671	7	NAO(t-27)	0.03061	19.06752
8	LSST(t-2)*LSST(t-35)	0.02462	-79.72197	8	NAO(t-16)*LSST(t-21)	0.02426	-41.07141
9	NAO(t-14)*LSST(t-41)	0.02155	-44.48801	9	SMB(t-33)*NAO(t-25)	0.02072	0.30667
10	NAO(t-28)*NAO(t-29)	0.01877	18.38886	10	LSST(t-29)*LSST(t-37)	0.01789	-58.94801
11	NAO(t-3)*LSST(t-37)	0.01893	35.81329	11	NAO(t-28)*NAO(t-37)	0.01708	18.53296
12	NAO(t-40)*NAO(t-46)	0.0152	-22.18935	12	NAO(t-28)*NAO(t-29)	0.01646	16.22431
13	NAO(t-7)*NAO(t-14)	0.0158	-22.95994	13	NAO(t-15)*LSST(t-29)	0.016	-39.75001
14	SMB(t-11)*NAO(t-38)	0.01249	0.34092	14	SMB(t-23)*NAO(t-13)	0.01302	0.38256
15	SMB(t-15)*NAO(t-27)	0.01058	0.32718	15	NAO(t-39)*NAO(t-47)	0.01138	16.57262

Acknowledgements

The authors would like to thank Michael Hicks from the IIP for providing the 2017 I48N data in advance of the Annual Report's publication. This work was motivated by the stimulation gained from the Second Workshop of the Glacial Ice Hazards Working Group, held in St. Johns, Newfoundland, in October 2017; the lead author wishes to thank the Chair, Ron Saper, for the invitation to the workshop. We acknowledge Philippe Huybrechts for contributing the original runoff model code, which EH used in adapted from to generate the monthly SMB timeseries. EH thanks the University of Sheffield Iceberg team, and particularly Mike Griffiths, for facilitating supercomputer access. We also thank NOAA, UCAR and ECMWF for allowing free access to data that were used within this study.

Disclosure Statement

No conflict of interest was reported by the authors.

Funding

This work was performed without specific funding.

References

- Barber DG, Babb DG, Ehn JK, Chan W, Matthes W, Dalman LA, Campbell Y, Harasyn ML, Firoozy N, Theriault N, Lukovich JV, Zagon T, Papakyriakou, Capelle DW, Forest A, Gariepy A. 2018. Increasing mobility of High Arctic sea ice increases marine hazards off the east coast of Newfoundland, *Geophys Res Lett*, doi:10.1002/2017GL076587.
- Bigg GR, Wei H, Wilton DJ, Zhao Y, Billings SA, Hanna E, Kadiramanathan V. 2014. A century of variation in the dependence of Greenland iceberg calving on ice sheet surface mass balance and regional climate change, *Proc Roy Soc Ser A*. 470: 20130662, doi:10.1098/rspa.2013.0662.
- Christensen E, Luzader J. 2012. From sea to air to space: a century of iceberg tracking technology. *Coast Guard Proc Mar Safety Sec Council*. 69: 17-22.

- Hanna E, Huybrechts P, Cappelen J, Steffen K, Bales RC, Burgess E, McConnell J, Steffensen JP, Van den Broeke M, Wake L, Bigg GR, Griffiths M, Savas D. 2011. Greenland Ice Sheet surface mass balance 1870 to 2010 based on Twentieth Century Reanalysis, and links with global climate forcing. *J Geophys Res Atmos.* 116: D24121.
- Hill BT. 2000. Database of ship collisions with icebergs. St. John's, Canada: Institute for Marine Dynamics, 36pp.
- Huntsberger DV, Billingsley P. 1973. Elements of statistical inference, 3rd edition. Allyn and Bacon, Boston.
- Hurrell JW, Deser C. 2009. North Atlantic climate variability, The role of the North Atlantic Oscillation. *J Mar Sys.* 78: 28-41.
- International Ice Patrol. 2017. Report of the International Ice Patrol in the North Atlantic Season of 2017. CG-188-72, US Coast Guard.
- Janssens I, Huybrechts P. 2000. The treatment of meltwater retention in mass-balance parameterizations of the Greenland ice sheet. *Ann Glaciol.* 31: 133 – 140.
- Kaplan A, Cane M, Kushnir Y, Clement A, Blumenthal M, Rajagopalan B. 1998. Analyses of global sea surface temperature 1856-1991. *J Geophys Res Oceans.* 103: 18567-18589.
- Marsh R, Bigg GR, Zhao Y, Martin M, Blundell J, Josey S, Hanna E, Ivchenko V. 2017. Prospects for seasonal forecasting of iceberg distributions in the North Atlantic. *Nat. Hazards*, <https://doi.org/10.1007/s11069-017-3136-4>.
- Murphy DL, Cass JL. 2012. The International Ice Patrol – safeguarding life and property at sea. *Coast Guard Proc Mar Safety Security Council.* 69: 13–16.
- Wilton DJ, Bigg GR, Hanna E. 2015. Modelling twentieth century global ocean circulation and iceberg flux at 48°N: implications for west Greenland iceberg discharge. *Prog Oceanogr.* 138: 194-210.
- Zhao Y, Bigg GR, Billings SA, Hanna E, Sole AJ, Wei H, Kadirkamanathan V, Wilton DJ. 2016. Inferring the variation of climatic and glaciological contributions to West Greenland iceberg discharge in the Twentieth Century. *Cold Reg Sci Technol.* 121: 167-178.
- Zhao Y, Hanna E, Bigg GR, Zhao Y. 2017. Tracking nonlinear correlation for complex dynamic systems using a Windowed Error Reduction Ratio method, *Complexity.* 2017: 8570720, doi:10.1155/2017/8570720.

Table 1. Observed I48N iceberg numbers and Case A mean ensemble predictions for 1997-2016, for cumulative totals from January to May (5 months) and September (9 months) respectively.

year	I48N May	Pred. May	I48N Sep.	Pred. Sep.
1997	885	241	1011	311
1998	1118	470	1380	646
1999	14	146	22	251
2000	737	219	843	254
2001	85	324	89	358
2002	813	104	877	215
2003	841	297	927	385
2004	138	137	262	268
2005	11	52	11	138
2006	0	225	0	265
2007	115	123	324	241
2008	930	320	976	517
2009	1002	217	1204	350
2010	0	124	1	293
2011	3	394	3	472
2012	485	364	499	731
2013	13	301	13	422
2014	1356	274	1546	574
2015	831	262	1161	427
2016	570	303	687	557
Mean	497.4	244.9	591.8	383.8
Std. dev.	458.6	107.4	528.4	157.4

Table 2. Ranking of observed and predicted (Case A) May and September I48N values and their categorisation as above (H) or below (L) the respective means given in Table 1.

year	Obs. May	H/L	Pred. May	H/L	Obs. Sep.	H/L	Pred. Sep.	H/L
1997	5	H	11	L	5	H	12	L
1998	2	H	1	H	2	H	2	H
1999	15	L	15	L	15	L	17	L
2000	9	H	13	L	9	H	16	L
2001	14	L	4	H	14	L	10	L
2002	8	H	19	L	8	H	19	L
2003	6	H	8	H	7	H	9	H
2004	12	L	16	L	13	L	14	L
2005	17	L	20	L	17	L	20	L
2006	20	L	12	L	20	L	15	L
2007	13	L	18	L	12	L	18	L
2008	4	H	5	H	6	H	5	H
2009	3	H	14	L	3	H	11	L
2010	19	L	17	L	19	L	13	L
2011	18	L	2	H	18	L	6	H
2012	11	H	3	H	11	H	1	H
2013	16	L	7	H	16	L	8	H
2014	1	H	9	H	1	H	3	H
2015	7	H	10	H	4	H	7	H
2016	10	H	6	H	10	H	4	H

Table 3. Observed I48N iceberg numbers and Case B mean ensemble predictions for 1997-2016, for cumulative totals from January to May (5 months) and September (9 months) respectively.

year	I48N May	Pred. May	I48N Sep.	Pred. Sep.
1997	885	396	1011	467
1998	1118	648	1380	896
1999	14	199	22	343
2000	737	312	843	362
2001	85	379	89	444
2002	813	270	877	416
2003	841	593	927	677
2004	138	290	262	444
2005	11	179	11	326
2006	0	256	0	284
2007	115	206	324	322
2008	930	545	976	724
2009	1002	602	1204	797
2010	0	424	1	635
2011	3	469	3	549
2012	485	674	499	1001
2013	13	396	13	541
2014	1356	622	1546	940
2015	831	607	1161	803
2016	570	623	687	948
Mean	497.4	434.5	591.8	596.0
Std. dev.	458.6	169.2	528.4	237.1

Table 4. Ranking of observed and predicted (Case B) May and September I48N values and their categorisation as above (H) or below (L) the respective means.

year	Obs. May	H/L	Pred. May	H/L	Obs. Sep.	H/L	Pred. Sep.	H/L
1997	5	H	12	L	5	H	12	L
1998	2	H	2	H	2	H	4	H
1999	15	L	19	L	15	L	17	L
2000	9	H	14	L	9	H	16	L
2001	14	L	13	L	14	L	13	L
2002	8	H	16	L	8	H	15	L
2003	6	H	7	H	7	H	8	H
2004	12	L	15	L	13	L	14	L
2005	17	L	20	L	17	L	18	L
2006	20	L	17	L	20	L	20	L
2007	13	L	18	L	12	L	19	L
2008	4	H	8	H	6	H	7	H
2009	3	H	6	H	3	H	6	H
2010	19	L	10	L	19	L	9	H
2011	18	L	9	H	18	L	10	L
2012	11	H	1	H	11	H	1	H
2013	16	L	11	L	16	L	11	L
2014	1	H	4	H	1	H	3	H
2015	7	H	5	H	4	H	5	H
2016	10	H	3	H	10	H	2	H

Table 5. The Case B WERR model predictions for 2017 and 2018. The mean values for I48N were calculated over 1997-2016 and 2017 observations are from IIP (2017).

Predicted values are given in whole numbers and all numbers show accumulations from January to the respective month. The months used for the verification comparison are shown in bold.

month	I48N	2017 pred	2017 obs	2018 pred
JAN	0	5±10	0	22±23
FEB	4	30±28	11	53±29
MAR	108	234±98	293	216±58
APR	281	407±231	676	381±136
MAY	498	590±267	882	559±180
JUN	577	687±287	981	650±187
JUL	591	734±295	997	658±193
AUG	592	764±296	1004	683±208
SEP	592	766±297	1008	685±207

Table 6. Ensemble members for predictions using Case B models for 2017 and 2018.

Ensemble members 1-11 are generated by models from the 30 year sliding windows from 1977-2006 through 1987-2016 respectively. Mean used in lower row is Case B verification mean given in Table 3.

member	May-17	Sep-17	May-18	Sep-18
1	86	196	297	448
2	237	354	285	330
3	423	468	372	459
4	934	990	752	863
5	637	1048	525	668
6	842	939	544	688
7	747	988	579	786
8	833	975	634	808
9	519	730	604	612
10	356	681	747	886
11	744	977	811	991
No. > mean	7	8	8	8

Figure 1. Schematic map showing main iceberg routes in the NW Atlantic (with arrows). The typical iceberg limit is shown by a solid line, with a typical maximum, April, sea-ice limit shown by the bold dashed line. The 48°N line used in measuring the monthly iceberg flux is shown dotted. For reference, the location of the sinking of RMS *Titanic* in 1912 is shown by a '+'.

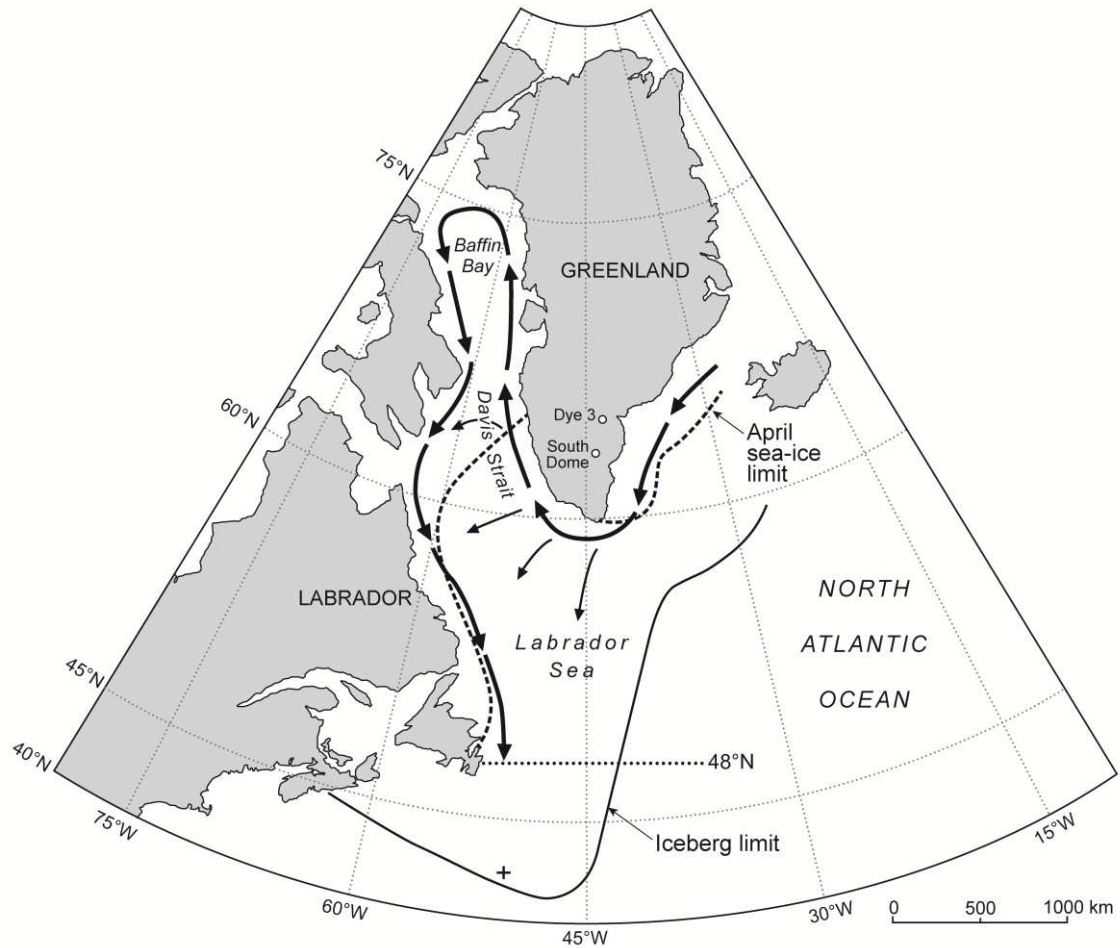


Figure 2. Icebergs crossing 48°N (I48N) during the period used in this study: a) annual total; b) mean monthly number.

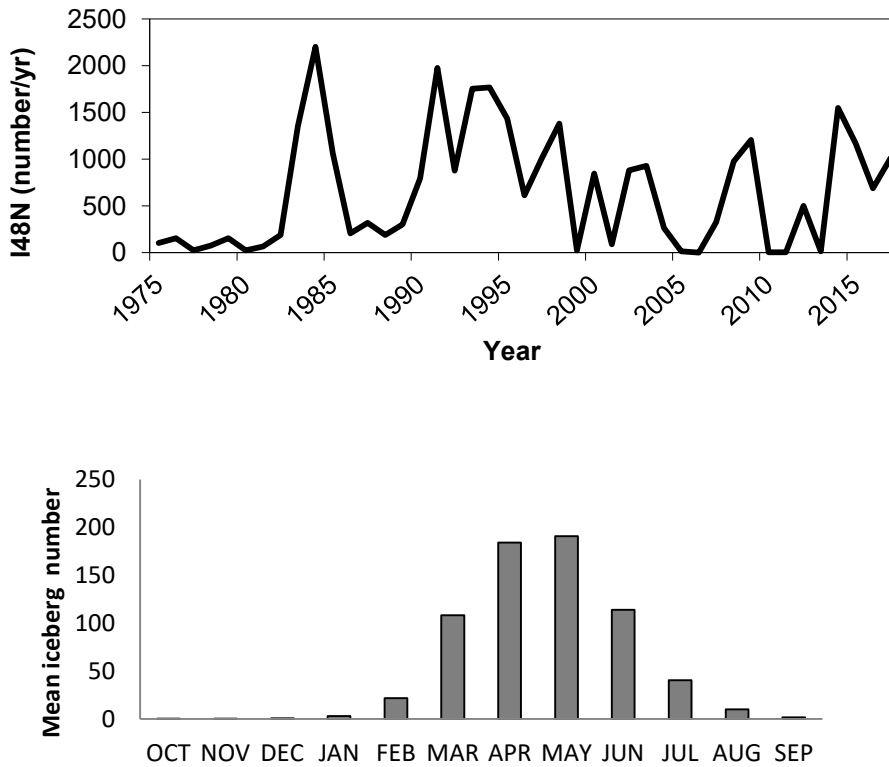


Figure 3. A comparison of the WERR monthly (red-dashed) and annual (blue dashed) model fits to the I48N (black) series, using the full suite of possible model terms. Taken from Figure 12 of Zhao et al. (2017). This is CC BY 4.0.

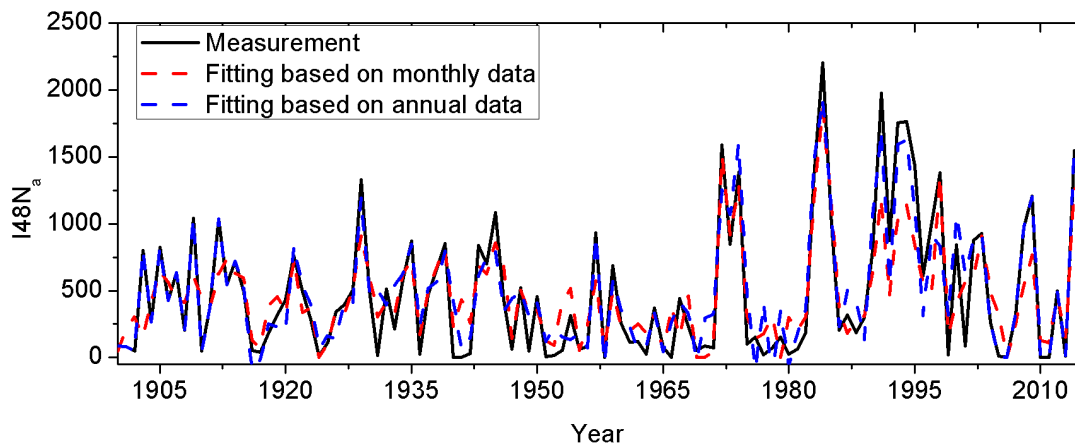


Figure 4. Distribution of September cumulative values of: (a) the I48N observations; (b) Case A; and (c) Case B predictions for the 1997-2016 period.

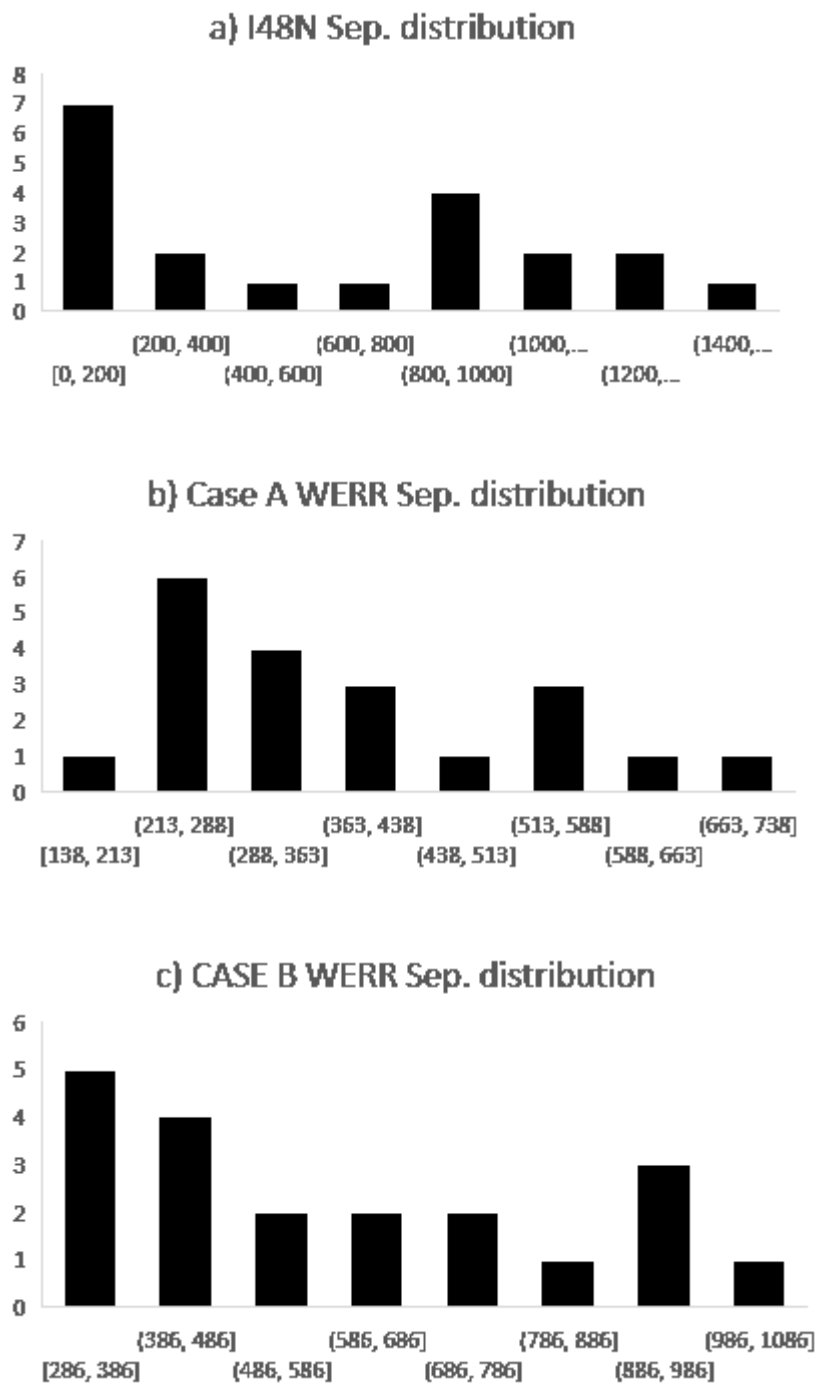


Figure 5. Cumulative I48N over January-September. The mean over 1976-2017 is shown (thick black line), as well as the actual observations for 2017 (black line). Predictions, with error bars, for 2017 (dashed) and 2018 (dotted) are shown dashed.

